Rev. Soc. cient. Parag. 2020;25(2):101-110

Gill B, Martínez-Pavetti B, Monteiro M. Chemical and microstructural characterization of blast furnace slag. Rev. Soc. cient. Parag. 2020;25(2):101-110.
https://doi.org/10.32480/rscp.2020.25.2.101
Recibido: 22/07/2020. Aceptado:15/10/2020.

ARTÍCULO ORIGINAL
ORIGINAL ARTICLE

Chemical and microstructural characterization of blast furnace slag

Caracterización química y microestructural de escoria de alto horno

Blanca Gill[1], Belén Martínez-Pavetti[2], Magna Monteiro[1*]

[1] Universidad Nacional de Asunción, Facultad Politécnica. San Lorenzo, Paraguay.
[2] Centro de Investigación en Matemática, Laboraotorio de Ecomateriales. Asunción, Paraguay.

Corresponding author: mmonteiro@pol.una.py

Abstract: Blast furnace slag is a byproduct of iron and steel production, whose physicochemical characteristics are influenced by the type of production process applied. Furthermore, its chemical composition depends on the raw materials used, the most common ones being mineral iron, coke and limestone. Blast slag can solidify into four different forms: crystallized, granulated, pelletized and expanded. Crystallized slag obtained from blast furnace production was studied in this work. This slag has high porosity and reduced mechanical strength when compared to other slags. The samples were submitted to thermal treatment at 860, 960 and 1060 ˚C for one hour. These samples were characterized by X-ray diffraction (XRD), infrared spectrometry (FTIR), X-ray Fluorescence (XRF) and scanning electronic microscopic/EDS. Based on the results, it was possible to predict the behavior of crystallization of the slag at different calcination temperatures and identify the present phases at each temperature range. This work aimed to characterize the blast furnace slag residue from steel production from Acepar Company S.A., in order to propose a higher added value application related to advanced ceramics production.

Keywords: characterization, blast furnace slag, thermal treatment, ceramic.

Resumen: La escoria de alto horno es un subproducto de la producción de hierro y acero, cuyas características fisicoquímicas están influenciadas por el tipo de proceso de producción aplicado. Además, su composición química depende de las materias primas utilizadas, siendo las más comunes el mineral de hierro, el coque y la piedra caliza. La escoria puede solidificarse en cuatro formas diferentes: cristalizada, granulada, *pelletized* y expandida. La escoria cristalizada obtenida de la producción de altos hornos se estudió en este trabajo. Esta escoria tiene una alta porosidad y una resistencia mecánica reducida en comparación con otras escorias. Las muestras fueron sometidas a tratamientos térmicos a 860, 960 y 1060 °C por una hora. Estas muestras fueron caracterizadas por difracción de rayos-X (XRD), espectrometría de infrarrojos con transformada de Fourier (FTIR), fluorescencia de rayos-X (XRF) y microscopia electrónica de barrido/EDS. Con base en los resultados, fue posible predecir el comportamiento de la cristalización de la escoria a diferentes temperaturas de calcinación e identificar las fases presentes en cada máximo de temperatura. Este trabajo tuvo como objetivo caracterizar la escoria de alto horno, residuo de la producción de acero de la Compañía Acepar, con el fin de proponer una aplicación de mayor valor agregado, relacionada con la producción de cerámicas avanzadas.

Palabras clave: caracterización, escoria de alto horno, tratamiento térmico, cerámica.

1. INTRODUCTION

Recycling of industrial waste is not only a need to maintain and protect the environment. The waste recycling process goes beyond adding value, also including the possibility of reducing the activities of exploitation of raw materials at the risk of scarcity and, very importantly, avoiding environmental devastation.

Blast furnace slag is a byproduct of iron and steel production. Its physicochemical characteristics are influenced by the type of production process used. Depending on the iron and steel production processes and the raw materials, the chemical composition and solidification structure of the blast slag can vary. Blast slag can solidify into four different structures: crystallized, granulated, pelletized and expanded. The crystalized slag, object of this study, is obtained by slow cooling of the liquid slag, that solidifies basically on silicates, aluminosilicates and calcium-alumina-silicates[1], with high calcium concentration.

Even if the blast furnace slag is classified as a residue, its application as a raw material is evident in several industrial sectors. Increasingly, it has been

drawing the attention of the researchers for the development of new applications and it is being considered as an environmental-friendly material[2]. Some applications of the slag in the industrial sectors are as complex fertilizer[1], glass–ceramic foams using waste slag and glass as raw materials[3], hydrothermal synthesis of zeolite[4] and adsorbent materials[5-8].

In this work, the samples of blast furnace slag, obtained from Aceros del Paraguay S.A. - Acepar, where the steel was processed by thermal treatment at different temperatures. This intends to determine if it is possible to utilize blast slag in an application of industrial level. The samples treated were characterized by X-ray diffraction (XRD), infrared spectrometry (FTIR) and scanning electronic microscopic (SEM/EDS). Based on the results, it was possible to predict the crystallized structure of the slag at different calcination temperatures, and the phases formed at each temperature. In addition, it was possible to confirm that this slag is adequate to be applied as heavy metal adsorbent and in vitroceramics production.

2. MATERIAL AND METHODS

The slag samples were collected from Acepar Company S.A., Paraguay, where steel production involves a coal-fueled blast furnace. Samples consists of slag discarded by the company. These samples were crushed with an agate mortar.

Then, samples were divided into four parts; three for thermal treatments at 860, 960 and 1060 °C, respectively, for 1 hour, with a heating rate of 10 °C/min, and the fourth part was preserved without any treatment (NC) as blank sample. The four samples were analyzed, in order to verify the changes and for quantification of the crystalline phases at the different temperatures. In addition, it was performed the evaluation of the chemical composition of each product obtained.

X-ray diffraction patterns of the samples were collected using a X'pert3 Powder, (Malvern Panalytical, Netherlands) with a CuKα radiation, generated at 45 kV and 40 mA, with CuKα source, 2θ range of 10 to 90°, the step size was 0.01° and step time of 0.5 s. Samples identification was made by comparing diffraction pattern with the ICDD (International Center for Diffraction Data) data bank.

Peak values of maximum intensities of each phase were used to determine their relative fractions. These values were calculated by the Eq. (a), which is the *Relative Intensity Ratio* (RIR) equation, presented below:

$$RIR_{phase\ 1..n} = \frac{I_{phase\ 1}}{\sum I_{phase\ 1..n}} \quad \text{(a)}$$

where, $I_{phase\ 1}$ is the maximum intensity of the phase considered and $\sum I_{phase\ 1..n}$ is the summation of the maximum intensities of all the phases identified in the sample which was being analyzed.

Fourier transform middle-infrared spectra of the samples in KBr pellets were recorded in the range 4000–400 cm^{-1} using a Thermo Scientific Nicolet iS5 vacuum spectrometer comprising an ATR accessory and an air-cooled DTGS detector (Thermo Fisher, USA). The spectra were recorded at a resolution of 4 cm^{-1} with 128 scans. This method was used to identify the vibrational bands of functional groups.

Scan electronic microscopy with electron dispersive spectroscopy detector, (EVO-15, Zeiss, German) was used to study the surface morphologies of the samples, and their chemical composition. For the analysis, all the samples were coated in vacuum with a layer of 8 nm gold plasma, conductive coating, to completely eliminate the charge effect. The microscopic images were taken up with 1.00 and 5.00 kx of magnitude, high vacuum with 15kV.

3. RESULTS AND DISCUSSION

The chemical compositions of heat-treated and blank slag samples are presented in Table 1. All the samples showed high content of calcium and silicon. The amount of calcium increases along with the temperature rise, and the concentration of other elements decreases with it. The slag with the highest calcium content (40.46% in mass) reported in the literature is employed for lead (II) adsorption [9]. In this case, the high calcium content favors the process of capture of heavy metals, since these tend to replace calcium in the crystal structure of the adsorbent[10].

Figure 1 shows the results of the XRD analysis of the starting slag (NC) and those from the thermally treated samples at 860, 960 and 1060 °C. The starting slag used for the processing of the samples is a crystallized slag, cooled to reach room temperature. This sample is amorphous with some crystalline phases, perhaps due to its cooling process. It can be observed in the XRD patterns of the heat-treated sample at 860 °C a small amorphous halo, which indicates that it still contains an amorphous phase, although its crystallinity is already more noticeable. In the samples processed at 960 and 1060 °C the amorphous halo is no longer observed and these samples are practically crystalline.

Table 1. Chemical composition of the blast furnace slag samples from Acepar, Paraguay, at different temperatures

Oxides (% wt)	Calcination temperature (°C)			
	Natural	860	960	1060
CaO	56.760	62.478	62.514	63.136
SiO_2	24.989	19.630	19.410	19.943
Al_2O_3	6.644	8.668	8.331	6.871
K_2O	5.462	4.325	4.371	3.943
MnO	0.356	1.837	1.829	1.829
FeO	3.237	1.602	1.734	2.301
BaO	1.476	-	0.679	0.930
TiO_2	0.604	0.791	0.529	0.443
SO_3	0.307	0.395	0.372	0.354
Sr	0.142	0.182	0.182	0.197
Ag	--	0.047	--	--
Zr	--	0.033	0.034	0.036
Y	0.016	0.010	0.011	0.012
*L.O.I		0.274	0.231	0.250

*Loss on ignition.

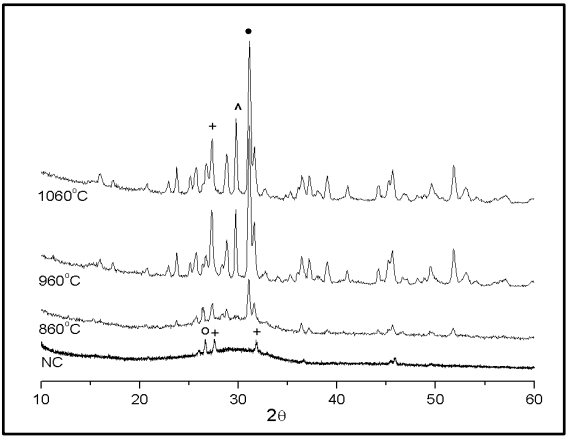

Figure 1. X-ray diffraction pattern for the blast furnace slag at different temperatures. (o) Quartz; (+) calcium silicate; (^) iron oxide; (•) calcium aluminum silicate.

The XRD spectrum of the sample thermally treated at 860 °C, shows a greater intensity of the peaks of the phases when compared to those present in the NC sample and the beginning of the formation of the calcium aluminum silicate phase, around 29.736 (2θ). The peaks of the phases observed in the

NC sample intensify as the temperature of the heat treatment is increased, and the crystallinity increases too, as observed in the spectra of the samples at 960 and 1060 °C. It is also likely to observe the loss of the peak that identifies the presence of quartz, the increment of calcium silicate phase and the appearance of a third phase corresponding to iron oxide. According to the chemical composition of the starting slag, it can be expected during the crystallization, the formation of the mineral groups pseudowollastonite (01-074-0874 - $Ca_3(Si_3O_9)$), magnatite (01-089-0951 - Fe_3O_4) and gehlenite (01-079-1726 - $Al_2Ca_2O_7Si$)[1,11], being the last one the predominant phase. Due to the great difficulty to identify the mineral phases, and the similarity in the patterns, with the eventual overlap or proximity of high intensity peaks, it is possible that leucite phase (01-085-1419 - $K(AlSi_2O_6)$) would be present.

The relative amount of each phase in the sample treated at 1060 °C was calculated by Eq. (a). From the XRD results, it can be verified that relative amounts of the principal phases are as follows: gehlenite (calcium aluminum silicate) 51.00%; magnetite (iron oxide) 25.00%; and pseudowollastonite (calcium silicate) 17.94%, this phase could also be considered as leucite (potassium aluminum silicate 01-085-1419), since both peaks have their maximum intensities very close.

Mihailova et al.[9] reported the formation of the merwinite phase containing magnesium, since the starting slag exhibited the presence of this element, indicated by the band around 617 cm^{-1}. Our FTIR data did not show such band, which corroborates the results of EDS analysis, for the composition of our starting slag. All bands identified in the spectrum of figure 2 are in concordance with the XRD results shown in Figure 1.

Figure 2 shows the FTIR spectra of the samples thermally treated at different temperatures. The NC sample presents little shoulders, which are related to the gehlenite minerals and calcium silicates. The sample treated at 860 °C presents a weak increase in the intensity of the band around 709 cm^{-1}, that can be related to the Si of the calcium silicate. The samples treated at 960 ºC and 1060 °C show progressive increase of the bands related to calcium silicate and gehlenite.

The sample treated al 960 °C shows a higher intensity of the 713 cm^{-1} band that corresponds to the symmetric vibrational of SiO_4 group, related to melilite groups; it can correspond to gehlenite mineral. Regarding the bands around to 800, 564, 859 and 646 cm^{-1}, the first two bands correspond to gehlenite and the last two correspond to larnite mineral, respectively. Furthermore, gehlenite bands occur at 851, 803 and 685 cm^{-1}, and a comparative analysis between spectra, let us possible to consider them as weak shoulder bands. The band around at 850 cm^{-1} represents a stretching of

Si-O bond from the tetrahedral silicate. The absorptions at 850-800 cm^{-1} appear in the characteristic frequency range of the interconnected AlO_4 polyhedral and due to the stretching vibrations of the Al-O-Al bonds. The band at ~680 cm^{-1} probably corresponds to a vibration stretching that primarily involves the movement of the Al with tetrahedral coordination.

In the sample treated at 1060 °C, the band around 715 cm^{-1} presents a higher intensity than those observed in the other samples. The shoulders of bands at 800 and 850 cm^{-1} increased weakly their intensity, and those bands representing the mineral gehlenite appear with greater intensity. It was also observed the occurrence of a new small band at 1030 cm^{-1}, corresponding to gehlenite, and the disappearance of the band at 475 cm^{-1} band corresponding to quartz.

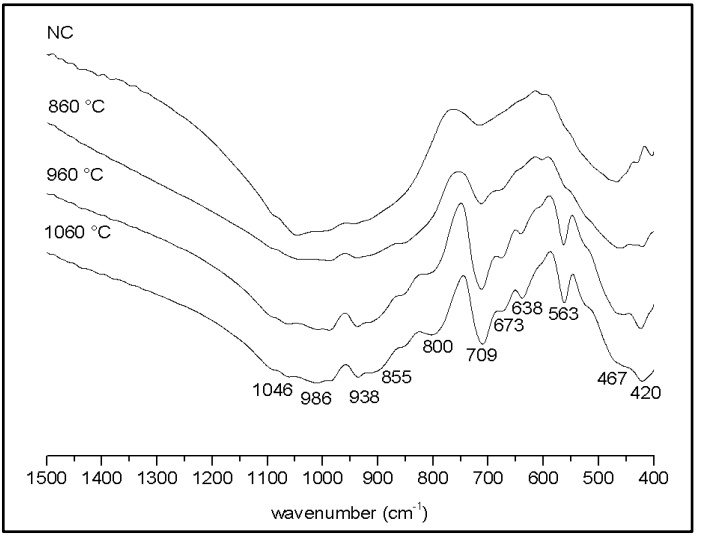

Figure 2. FTIR spectra for the blast furnace slag at different temperatures.

Microstructures of treated and untreated samples, revealed by scan electronic microscopy (SEM) are shown in Figure 3. It is possible to visualize morphology changes in the particles and their surfaces, depending on the thermal treatment applied. In Figure 3(a), it can be observed that the untreated samples present a quite rough and microporous surface, typically observed in this kind of slag[9], when compared to treated samples. Besides this, can be observed that as the temperature of thermal treatment increases, microporosity reduces, which might be directly related to the granule coalescence process, resulting in more compacted particles. Although sample

M2, Figure 3(b), presents particulate material on its surface, and is still possible to appreciate that it has a smoother and less rough surface, which might be associated to the beginning of formation of a new crystallographic phase, calcium aluminum silicate, Figure 1. Along with the temperature increase, this phase also increases considerably, resulting in samples M3 and M4, Figure 3(c) and (d), calcinated at 960 °C and 1060 °C, respectively, exhibiting both of them a smooth and rounded surface, being almost free of microporosities.

Magnification	
1.00 kx	5.00 kx
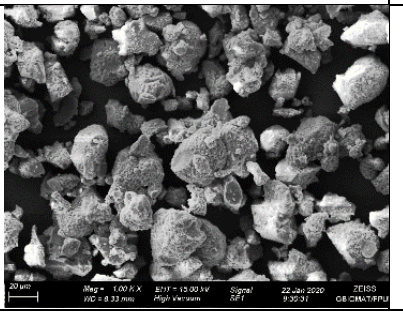	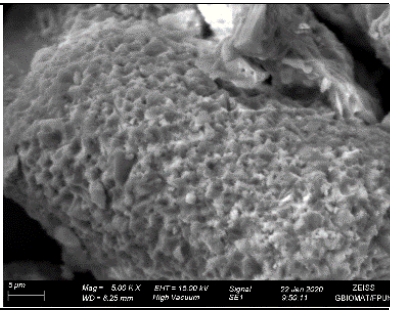
(a) M1 – NC	
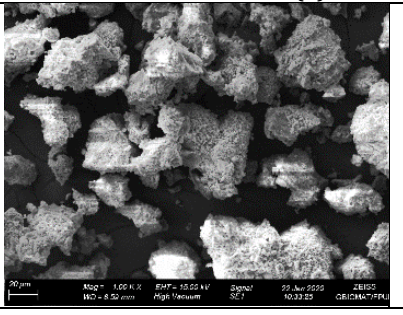	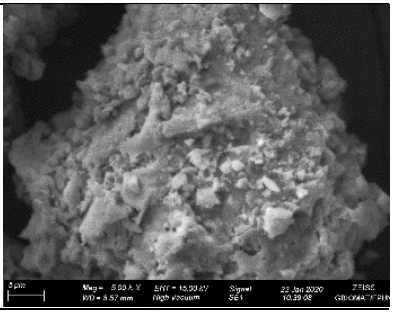
(b) M2 – 860 °C	

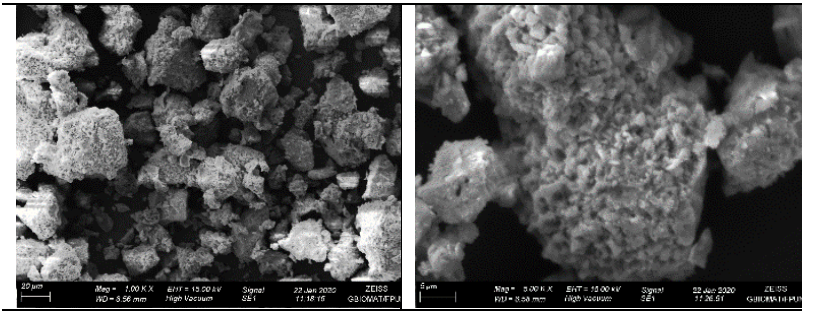

(c) M3 – 960 °C

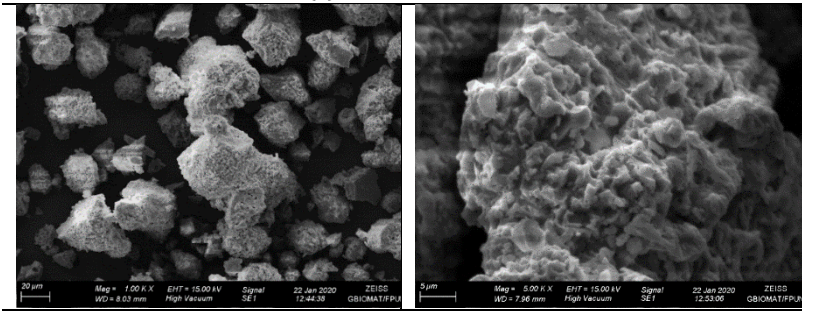

(d) M4 – 1060 °C

Figure 3. SEM analysis of the samples.

4. CONCLUSIONS

The results obtained from the characterization of blast furnace slag treated at different temperatures show that the samples have high content of calcium. The samples treated at 960 and 1060 °C exhibited mainly calcium aluminum silicate and gehlenite mineral, which favors the application of slag as heavy metal adsorbent and vitroceramic production. These results encourage us to continue our research work directed to explore the subsequent application of the slag as raw material in environmentally friendly applications.

REFERENCES

1. Maghchiche A, Naseri R, Haouam A. Uses of Blast Furnace Slag as Complex Fertilizer. J. Chem. Chem. Eng. 2012; 6: 853-859.
2. Quintana HAR, Farias MMF, Lizcano FAR. 2018. Uso de escorias de alto horno y acero en mezclas asfálticas: revisión. Rev Ing Uni Medellín. 2018; 17 (33): 71 - 97.

3. Ding L, Ning W, Wang Q, Shi D, Lou L. 2015. Preparation and characterization of glass-ceramic foams from blast furnace slag and waste glass. Mater Lett. 2015; 141:327-329.
4. Sugano Y, Sahara R, Murakami T, Narushima Y, Ouchi C. 2015. Hydrothermal synthesis of zeolite a using blast furnace slag. ISIJ Int. 2015; 45(6): 937-945.
5. Nilforoushan MR, Otroj S, Talebian N. The Study of Ion Adsorption by Amorphous Blast Furnace Slag. Iran. J Chem Chem Eng. 2015; 34(1): 57-64.
6. Jha VK, Kameshima Y, Nakajima A, Okada K. Utilization of steel-making slag for the uptake of ammonium and phosphate ions from aqueous solution. J Hazar Mater. 2008; 156: 156–162.
7. López FA, Martín MI, Pérez C, López-Delgado A, Alguacil FJ 2003. Removal of copper ions from aqueous solutions by a steel-making by-product. Water Res. 2003; 37: 3883–3890.
8. Ortiz N, Pires MAF, Bressiani JC. Use of steel converter slag as nickel adsorber to wastewater treatment. Waste Manage, 2001; 21: 631-635.
9. Mihailova I, Dimitrova S, Mehandjiev D. 2013. Effect of the thermal treatment on the Pb(II) adsorption ability of. J Chem Tech Metall. 2013; 48(1): 72-79.
10. Ellis DE, Terra J, Warschkow O, Jiang M, González GB, Okasinski JS, Bedzyk MJ, Rossi AM, Eon JG. A theoretical and experimental study of lead substitution in calcium hydroxyapatite. Phys Chem Chem Phys. 2006; 8: 967-976.
11. Taylor WR. Application of infrared spectroscopy to studies of silicate glass structure: Examples from the melilite glasses and the systems Na20-SiO2 and Na20-AI203-SiO2. Proc Indian Acad Sci (Earth Planet. Sci.). 1990; 99 (1): 99-117.